AIMS Materials Science, 8(3): 321–342.
DOI: 10.3934/matersci.2021021
Received: 30 March 2021
Accepted: 16 May 2021
Published: 26 May 2021

http://www.aimspress.com/journal/Materials

*Research article*

# Copper matrix composites reinforced with steel particles

**Marcin Kargul*, and Marek Konieczny***

Department of Metals Science and Materials Technologies, Kielce University of Technology, Kielce, Poland

* **Correspondence:** Email: mkargul@tu.kielce.pl, mkon@tu.kielce.pl.

**Abstract:** The paper presents the results of research on the production and application of sintered copper matrix composites reinforced with carbon steel and T15 HSS steel particles. The starting materials for obtaining the sintered composites were commercial powders of copper, carbon steel and T15 HSS steel. Experiments were carried out on specimens containing 2.5, 5, 7.5, and 10% of steel particles by weight. Finished powder mixtures containing appropriate quantities of steel were subjected to single pressing with a hydraulic press at a compaction pressure of 624 MPa. Obtained samples were subjected to a sintering process in a sillit tubular furnace at 900 °C in an atmosphere of dissociated ammonia. The sintering time was 2 h. After the sintering process, the samples were cooled in a cooler mounted in the furnace. The obtained sinters were subjected to hardness, density, electrical conductivity, and abrasion resistance measurements. Observations of the microstructure of metallographic specimens made from the sintered compacts were also performed using an optical microscope and scanning electron microscope (SEM). After the abrasion resistance tests, the geometric structure of the surface was observed. The hardness increased in comparison with a sample made of pure copper, whereas the density and electrical conductivity decreased. The highest hardness was obtained for the composite containing 10% of T15 high speed steel particles which amounted 61 HB. This is due to presence of carbides in the steel particles. The highest electrical conductivity was obtained for the composite containing 2.5% of T15 high speed steel which amounted 40 MS/m (68% of solid copper conductivity). Tribological tests have shown that the introduction of high-speed steel particles increases the abrasion resistance of composites.

**Keywords:** copper matrix composites; powder metallurgy; sintering; copper; carbon steel; HSS steel

## 1. Introduction

Currently, scientists around the world are conducting research on the production of modern materials with the desired properties. In essence, a single material does not have high satisfactory properties, therefore composites, i.e., materials consisting of at least two phases with different properties, play an increasingly important role in the industry. In recent years, sintered copper matrix composites are finding an increasing interest. Copper is widely used for the production of electrical and electronic devices due to its high electrical conductivity, corrosion resistance, low cost, and easy production. Due to the high electrical conductivity of copper, electrical components such as relays, switches, electric motor components, and electrode tips for resistance welding are produced using powder metallurgy [1–6]. Pure copper has low hardness, mechanical strength, and abrasion resistance, which limits its use in a pure form. For this reason, pure copper is strengthened by introducing alloying additions. However, the introduction of any addition to copper reduces their electrical conductivity. For example, thin bronze, silicon bronze, and manganese bronze have an electrical conductivity lover less than 10 MS/m while pure copper has 59.7 MS/m [7]. To increase the strength properties of composites without significantly lowering the electrical conductivity, metal oxides ($Al_2O_3$, $SiO_2$, $ZrO_2$, $Cr_2O_3$, BeO, MgO, $TiO_2$), carbides (SiC, TiC, $Cr_7C_3$, $Cr_3C_2$), nitrides (TiN, BN) and borides ($TiB_2$, $ZrB_2$, $CrB_2$) are introduced into the copper matrix [8–16]. The introduction of the above-mentioned particles increases the strength properties and increases the resistance to abrasive wear. In addition to ceramic particles, metal particles are also introduced into the copper matrix, which together with the matrix form intermetallic phases. Sintered composites reinforced with intermetallic phases have properties similar to those of composites reinforced with ceramic particles. For the strengthening of sintered composites, copper-titanium, aluminium-iron, and nickel-aluminium intermetallic phases are most often used [17–21]. Metal matrix composites reinforced with strengthening particles are usually fabricated using powder metallurgy. The main advantage of powder metallurgy is a very good control over the distribution of strengthening particles in the matrix. An important role in powder metallurgy is the diffusion of the solid state dependent on sintering time and temperature, which is involved in the formation of intermolecular bonds. There is a lack of scientific work on the production of sintered composites with a copper matrix reinforced with steel particles. Steel particles are characterized by high hardness and resistance to abrasive wear, therefore introducing them into the matrix should significantly increase the strength properties of composites [22–25]. In this work, an attempt was made to produce sintered copper matrix composites reinforced with particles of carbon steel and high speed steel. The fabricated sinters were subjected to microstructural investigations and measurements of density, hardness, and electrical conductivity. The abrasive wear tests of the composites were also carried out and the geometric structure of the surface was observed. An abrasion resistance test was required to check that the copper-steel composites have the properties to apply it to the electric motor brushes. An electric brush is a special type of electrical contact between two or more moving parts. Usually the brushes work with a commutator or slip ring. Depending on the design requirements and the type of contact, the brush can be made of a metal alloy (e.g., with a high copper content) or a suitably prepared abrasion-resistant graphite [26]. The higher content of graphite has a positive effect on the smaller wear of commutators and rings. However, the material with a higher copper content is used at high current densities, in low voltage DC machines and high current, e.g., car starters. Brushes require constant pressure, the force of which is predetermined for a specific design solution. Due to

the constant contact of the electric brush with the commutator or the slip ring, the brushes wear out. There is therefore a need for a flexible electrical connection between the brush and the rest of the system. For this purpose, usually a braided copper rope is used, which allows the brushes to move freely. As the device is working, regular wear of brushes occurs, which from time to time must be changed into new ones [27]. Conducted tests predestine the produced sinters for the aforementioned use.

## 2. Materials and methods

Materials used in this experiment were copper powder (99.5%Cu), carbon steel powder (0.8%C), and high speed steel T15 powder. The chemical compositions of T15 steel powder used in the experiment are shown in Table 1. Electrolytic copper powder with an average particle size of less than 63 μm was used as the matrix, while steel powders with an average particle size of less than 200 μm was used as the reinforcement. The shapes and arrangements of the powder particles used in the experiments are shown in Figures 1–3.

**Table 1.** Composition of T15 HSS steel powder.

| | Chemical composition, %wt | | | | | | | |
|---|---|---|---|---|---|---|---|---|
| T15 HSS | C | Si | Mn | Cr | Mo | V | W | Co |
| | 1.5 | 0.4 | 0.4 | 4.5 | 0.5 | 5.0 | 12.5 | 4.75 |

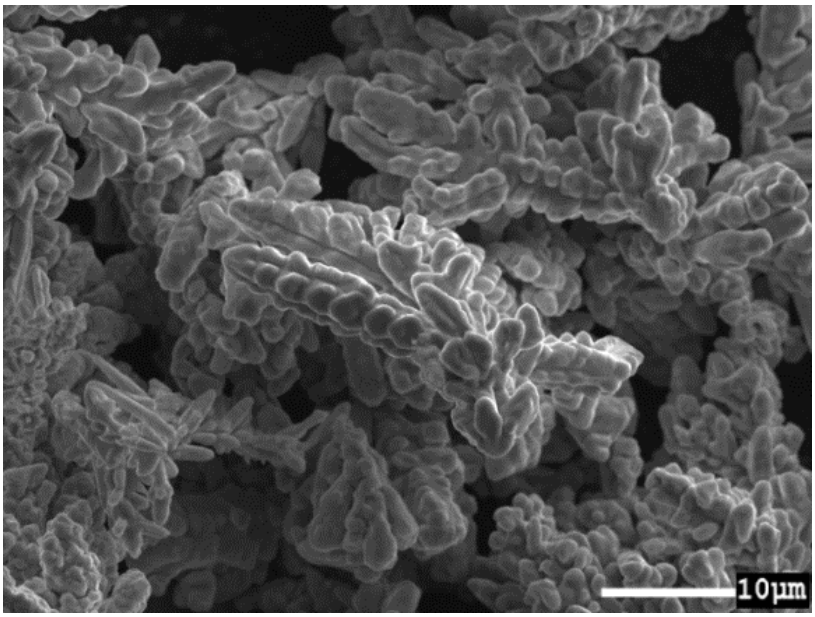


**Figure 1.** Electrolytic copper powder (SEM).

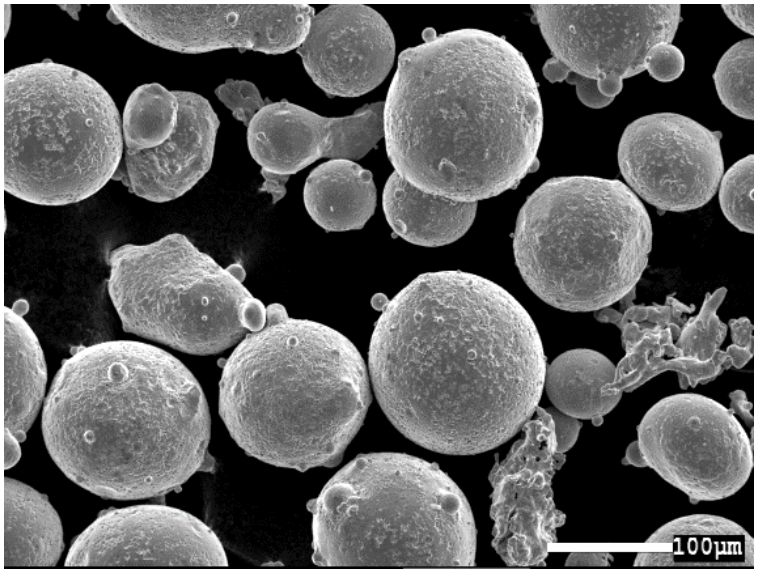


**Figure 2.** HSS T15 steel powder (SEM).

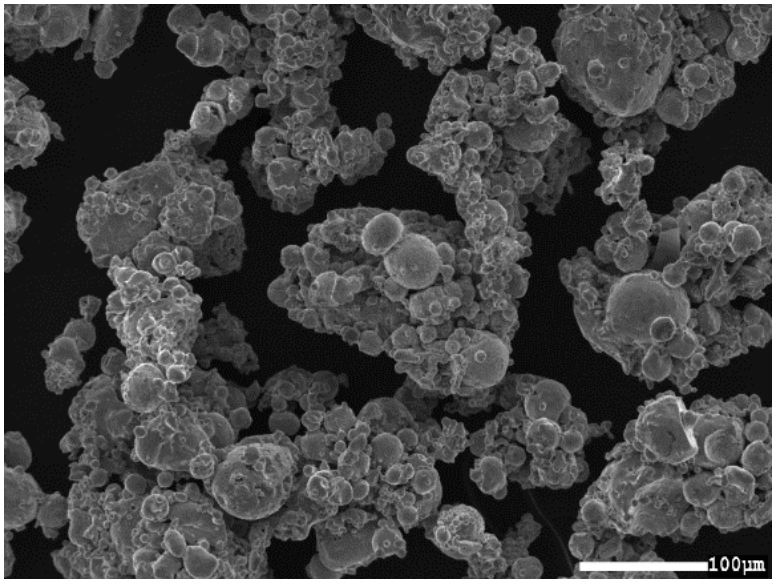


**Figure 3.** Carbon steel powder (SEM).

The powders of the materials used to fabricate the composites were observed using a JEOL JSM-7100F field emission scanning electron microscope. Two batches of powder mixtures were made, the first batch is a mixture of copper powder and carbon steel, while the second batch is a mixture of copper powder and T15 high speed steel powder. Powder mixtures with different steel powder content (2.5, 5, 7.5, and 10% by weight) were prepared for the tests. Cylindrical samples with a dimension of Φ20 × 10 mm were made of the prepared powder mixtures with a hydraulic press at a compaction pressure of 620 MPa. The specimens were sintered in a sillit tubular furnace at 900° in the dissociated ammonia atmosphere. The sintering time was 2 h. After the sintering process, the samples were subjected to cooling. The fabricated composites were subjected to hardness, density, electrical conductivity, and abrasion resistance tests. The hardness of the sintered compacts was measured using

the Brinell method (with a steel ball of 5 mm in diameter at a load of 2452.5 N) in accordance with the PN EN ISO 6506-1:2014 standard. Tests of electrical conductivity were carried out using the eddy current method using a GE Phasec 3D device. The density was determined by weighing the specimens in air and water using WPA120 hydrostatic scales in line with the PN EN ISO 2738:2001 standard. Microstructure analysis of the previously prepared metallographic specimens were conducted using the JEOL JSM-7100F field emission scanning electron microscope fitted with OXFORD INSTRUMENTS EDS X-Max Aztec software for elemental analysis. The abrasion resistance tests of the fabricated composites were conducted using a Anton Paar TRB3 ball-on-disc tribometer according to the requirements of the ASTM G 99 standard.

The following parameters were set for the test:

- Friction pair: a 100Cr6 steel ball (10 mm in diameter) and a disc made of copper with an addition of various amounts of steel particles (2.5–10% of steel particles);
- Load P = 5 N;
- Sliding velocity v = 0.1 m/s;
- Friction path distance s = 1000 m;
- Humidity 47 ± 1%;
- Ambient temperature $T_0$ = 22 ± 1 °C;
- Atmospheric pressure 987 ± 5 hPa.

Abrasive wear resistance test was carried out under dry friction conditions. The samples were weighed both before and after the tribological tests to determine the weight loss. Analyses of the geometric structure after the tribological tests were performed using a Leica DCM8 optical profilometer.

## 3. Results and discussion

### *3.1. Microstructural investigations*

The introduction of particles, both carbon steel and high-speed steel into the copper matrix caused significant changes in the microstructure of the composites. Particles of carbon and HSS steel of various shapes and sizes are clearly visible in the copper matrix. Differences in a particle size result from the range of the size of the introduced steel powders (<200 μm). The shape of the particles depends on the method of producing the powders. The steel powders were produced by the spraying method, as evidenced by the spherical shape of the powder. Due to the thorough mixing of the powders before the pressing process, an even distribution of particles in the copper matrix was achieved. In some areas, the particles aggregate into agglomerates. No large clusters of steel particles were observed. The steel particles did not dissolve in the copper matrix, which proves their high thermal resistance. There is no diffusion between the steel particles and the copper matrix, thanks to which the electrical conductivity is not significantly reduced. Exemplary microstructures of sintered copper-steel composites obtained using an optical microscope are shown in Figures 4 and 5.

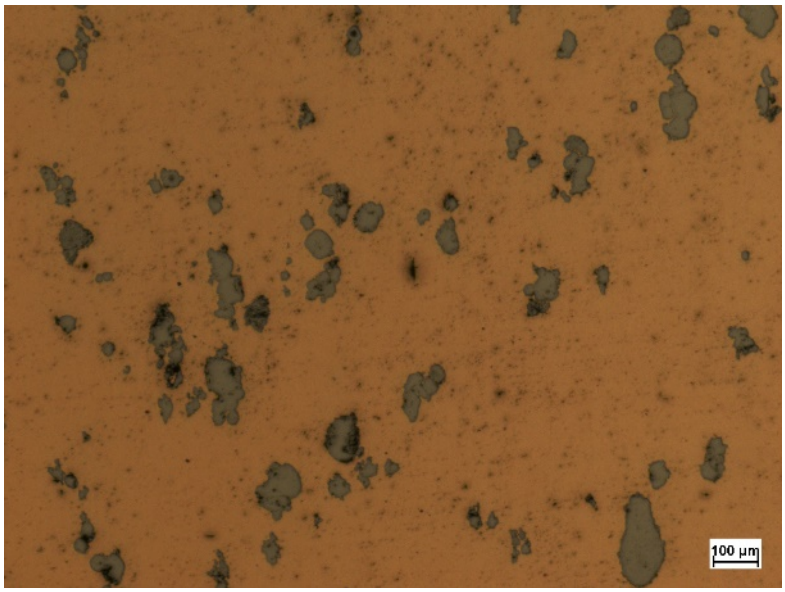


**Figure 4.** Microstructure of the sintered composite containing 5% of carbon steel.

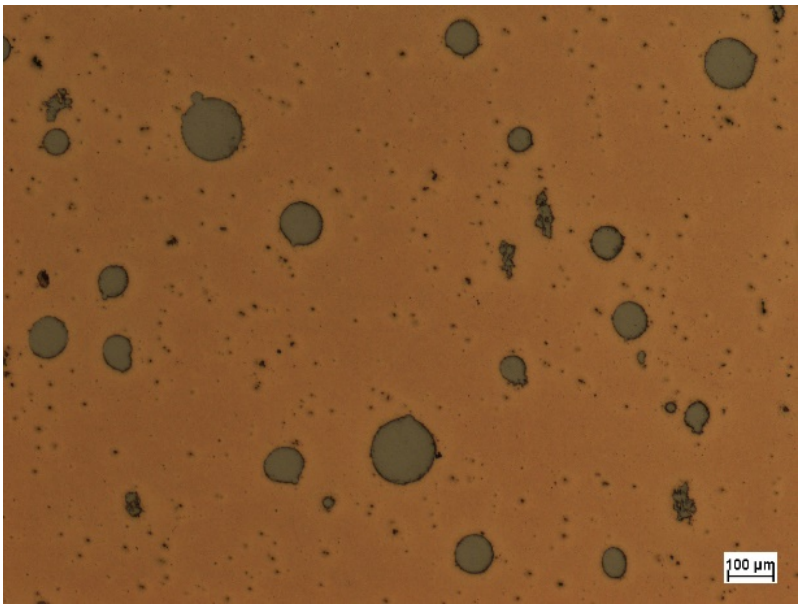


**Figure 5.** Microstructure of the sintered composite containing 5% of T15 HSS steel.

To reveal the microstructure of steel particles after sintering, the samples were subjected to an etching process. Nital was used as the etching agent. In the case of carbon steel with 0.8% carbon, the pearlitic structure is present. The annealed high-speed steel microstructure consists of a metal matrix composed of ferrite containing alloying elements and metal carbides. The high-speed steel structure includes $M_6C$ and MC types of carbides [25]. The carbides are visible in the microstructure of the steel as bright spots on the background of the metal matrix. Similar microstructures of steel were also shown by other researchers [22–24]. The microstructures of steel particles after sintering and etching are shown in Figures 6 and 7.

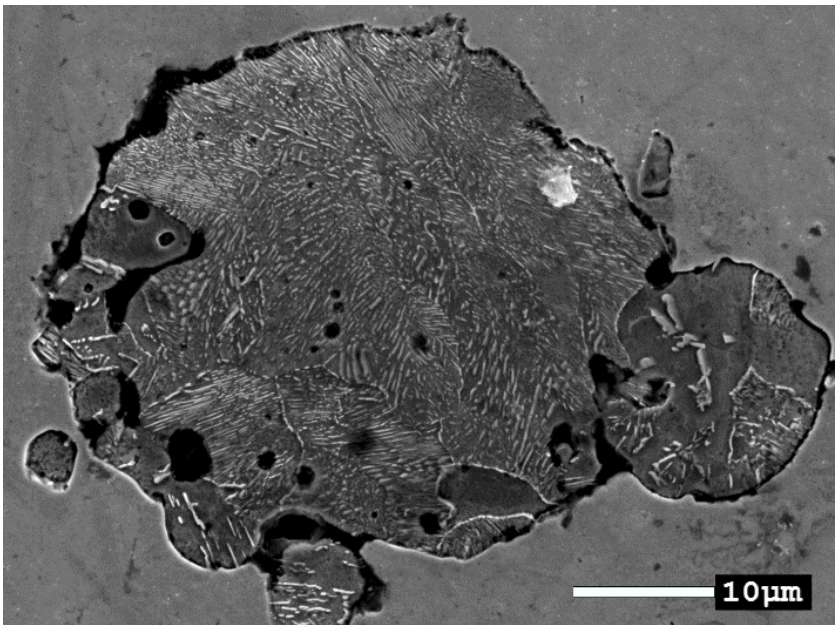


**Figure 6.** Microstructure of carbon steel particles after sintering.

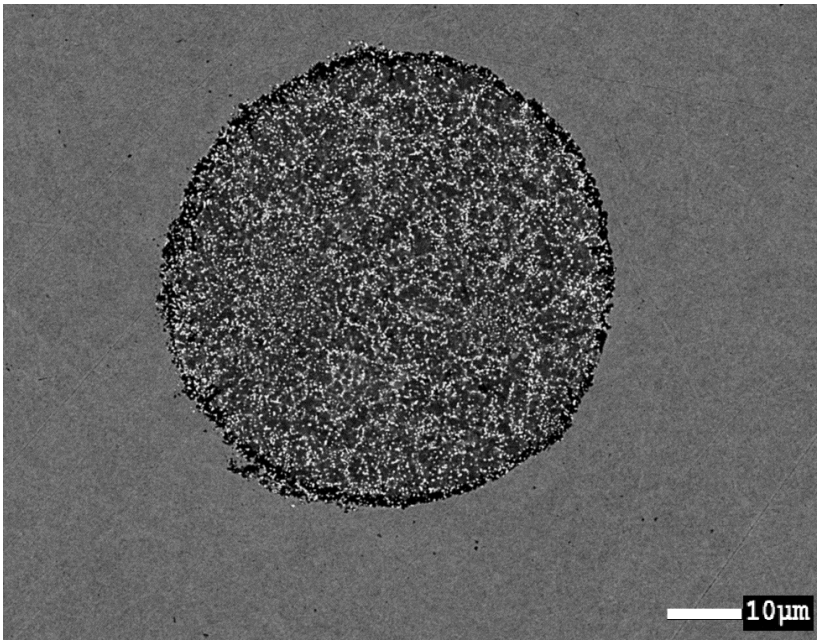


**Figure 7.** Microstructure of T15 HSS steel particles after sintering.

*3.2. Density and hardness measurements*

The hardness tests of the composites were carried out to assess how the amount of the introduced steel particles influences their hardness. The results of density and hardness measurements are presented in Tables 2 and 3.

**Table 2.** Results of density and hardness (HB) measurements of Cu-carbon steel particles.

| Material | Density (g/cm$^3$) | Relative density (%) | HB |
|---|---|---|---|
| Cu | 8.19 ± 0.02 | 92.01 | 36.65 ± 1.5 |
| Cu + 2.5% of 0.8%C | 8.00 ± 0.04 | 81.41 | 44.79 ± 1.8 |
| Cu + 5% of 0.8%C | 7.78 ± 0.05 | 90.65 | 52.36 ± 1.3 |
| Cu + 7.5% of 0.8%C | 7.22 ± 0.03 | 87.95 | 53.80 ± 1.7 |
| Cu + 10% of 0.8%C | 7.12 ± 0.07 | 82.10 | 56.83 ± 1.8 |

**Table 3.** Results of density and hardness (HB) measurements of Cu-T15 HSS steel particles.

| Material | Density (g/cm$^3$) | Relative density (%) | HB |
|---|---|---|---|
| Cu | 8.19 ± 0.02 | 92.01 | 36.65 ± 1.5 |
| Cu + 2.5% of T15 | 7.50 ± 0.04 | 75.09 | 43.68 ± 1.8 |
| Cu + 5% of T15 | 7.08 ± 0.05 | 78.05 | 46.33 ± 1.3 |
| Cu + 7.5% of T15 | 6.90 ± 0.03 | 79.91 | 57.36 ± 1.7 |
| Cu + 10% of T15 | 6.67 ± 0.07 | 84.94 | 61.26 ± 1.8 |

The examination showed that the introduction of both carbon steel and high-speed steel particles into the copper matrix resulted in a significant increase in the hardness of the composites and a decrease in their density. Increasing hardness of composites is related to the high hardness of steel particles. The hardness of carbon steel with 0.8% carbon content after annealing is about 200 HB, while the hardness of T15 high-speed steel is about 280 HB. The highest hardness was obtained for a composite containing 10% of T15 HSS steel particles which amounted 61 HB (67% higher than pure copper sinter). An increase in hardness with an increase in the amount of strengthening particles was also shown by other researchers [2,3]. The density of composites decreases with increasing amount of steel particles. This is due to the lower density of the steel particles compared to the copper matrix. The introduction of 10% of carbon steel particles by weight reduces the density to 7.12 g/cm$^3$ and to 6.67 g/cm$^3$ in the case of T15 HSS steel particles. Lowering the density of sintered composites are also shown by other researchers [4,5,8].

### *3.3. Electrical conductivity investigations*

The electrical conductivity tests of composites have shown that the introduction of a small amount of steel particles into the copper matrix causes a significant reduction in electrical conductivity in comparison with other reinforcements such as $TiB_2$ in spark plasma sintered Cu-$TiB_2$ composites [15]. The obtained results were compared with the results for the sintered copper powder. A sinter made of pure copper powder has an electrical conductivity of 50.39 MS/m (14% less than copper in a solid state). The introduction of carbon steel particles into the copper matrix significantly lowered the electrical conductivity. The addition of 2.5% reduced the electrical conductivity to 33 MS/m, while the addition of 10% of carbon steel particles reduced the electrical conductivity to 14 MS/m. Much better results were obtained for composites reinforced with T15 high-speed steel particles. The introduction of 2.5% of T15 steel particles lowered the electrical conductivity to less than 40 MS/m, while at the content of 10% to 24 MS/m. The relatively high electrical conductivity is due to the lack of diffusion between the copper matrix particles and the steel particles. As

reinforcement particles increased the electrical conductivity decreased. The main reason is related to the existence of pores which can be inferred from the density reduction. An important factor influencing the electrical conductivity is also the purity of the powders used in the experiment. The reduction of electrical conductivity with the increase of the amount of strengthening particles was also obtained for composites reinforces with $ZrB_2$ particles [11]. The results of electrical conductivity measurements are shown in Figures 8 and 9.

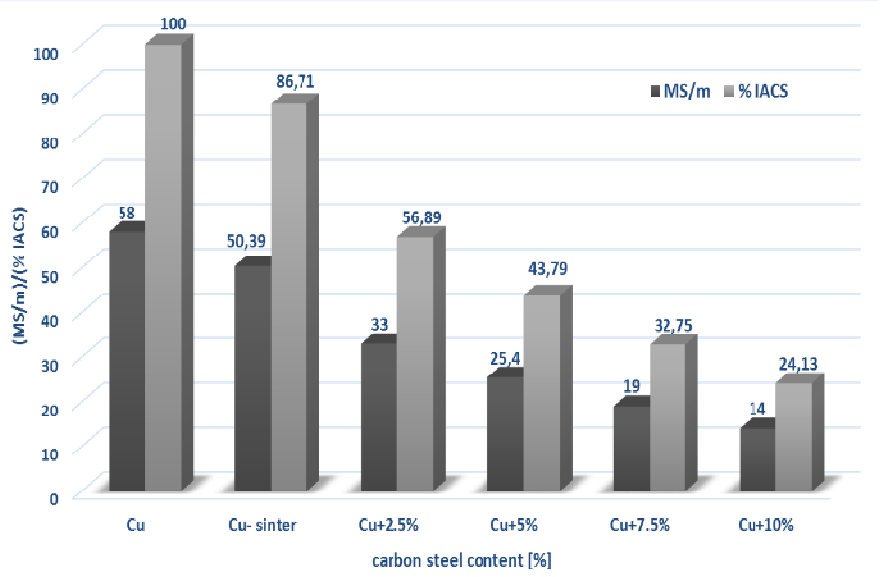


**Figure 8.** The results of electrical conductivity measurements of copper-carbon steel composites.

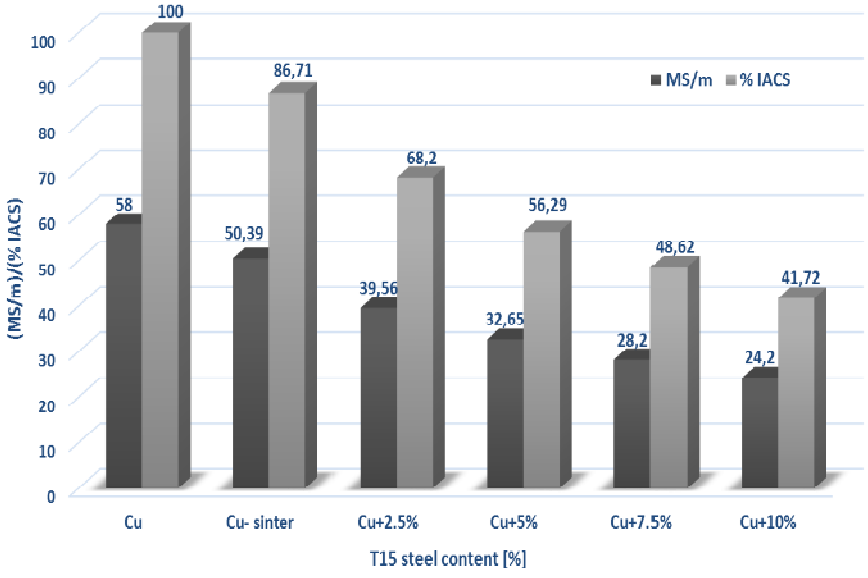


**Figure 9.** The results of electrical conductivity measurements of copper-T15 steel composites.

### *3.4. Wear characterization*

The samples for the abrasion resistance tests were weighed both before and after the tests to determine the weight loss. The parameters of the abrasive wear resistance tests are presented in the second chapter of this paper. The results were compared with a sample made of copper powder. The weight loss after abrasion resistance tests for a sample made of copper powder was 0.0123 g. The weight loss for samples reinforced with steel powders is shown in Figure 10.

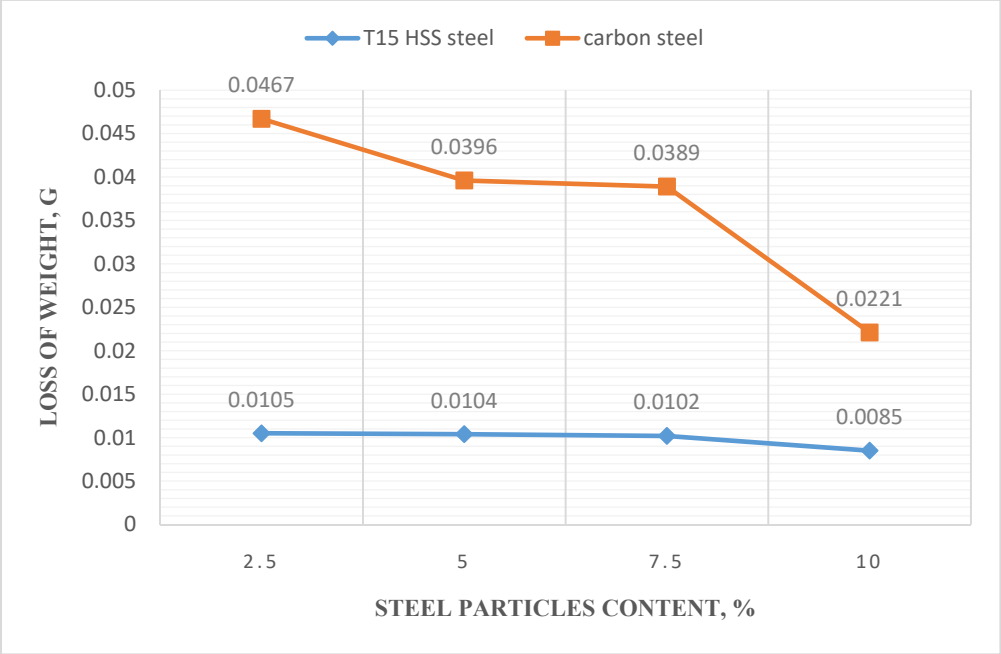


**Figure 10.** Weight loss of composites depending on the content of steel particles.

Tribological tests have shown that introducing high-speed steel powder as reinforcing particles into the copper matrix increases the abrasion resistance. This may be due to the high wear resistance of the T15 high-speed steel particles. In the case of carbon steel particles, the weight loss of composites is much greater than in the case of a sample made of copper powder. Less abrasive wear of composites reinforced with T15 high speed steel particles may be due to the shape of the particles and a better bond with the copper matrix. Other researchers have also obtained an increase in the wear resistance of copper matrix composites reinforced with particles [26,27].

After carrying out the tribological tests, the geometric structure of the composites surface was observed using an optical profilometer. The figures below show the surface texture topography after tribological tests, where it possible to observe the abrasion trace and the way the particles were torn out of the copper matrix. The profiles of the surface cross-section are also presented in order to accurately observe the depth and shape of the wear. The geometric structures of the composites with various amounts of steel particles after tribological tests are shown in Figures 11–19.

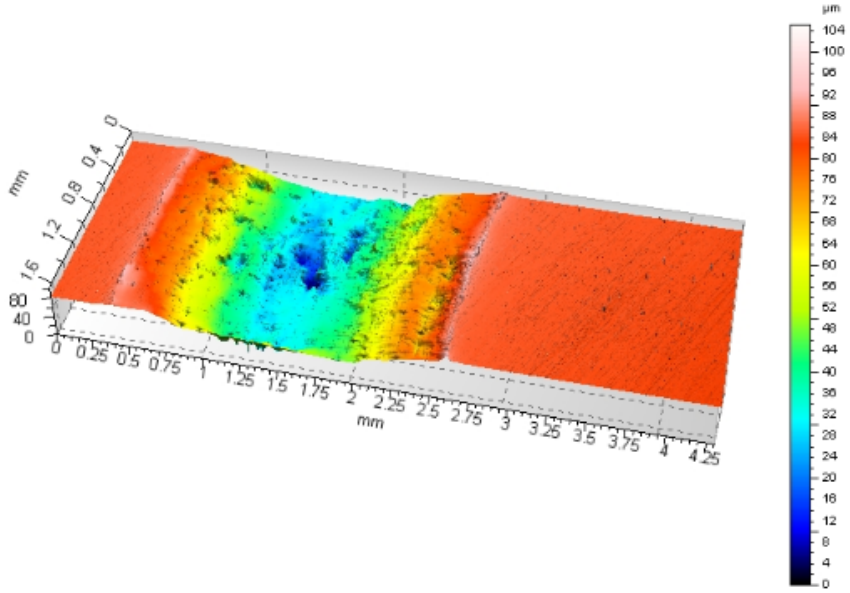


(a)

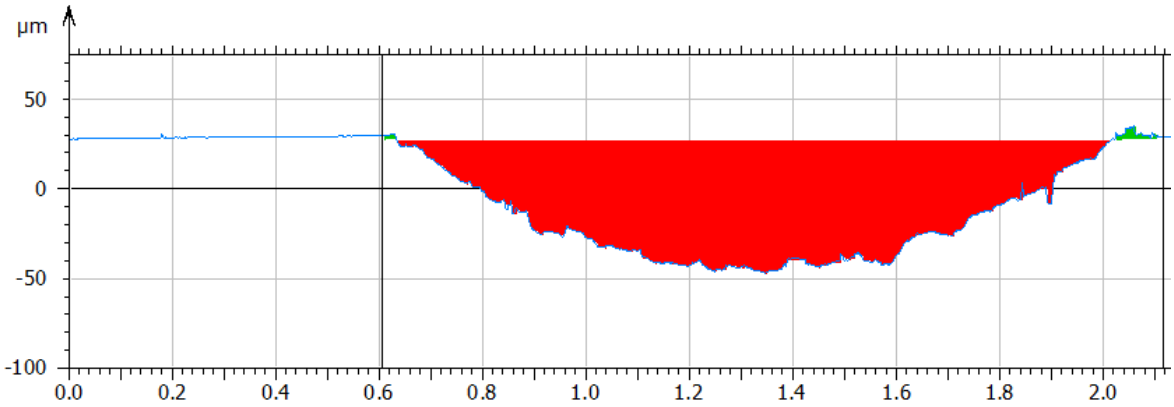


| Parameters | Value | Unit |
|---|---|---|
| Maximum depth | 73.61 | µm |
| Hole area | 74642 | µm² |

(b)

**Figure 11.** Surface texture topography of the composite made of pure copper after tribological tests under technically dry friction: (a) isometric image, (b) surface profile.

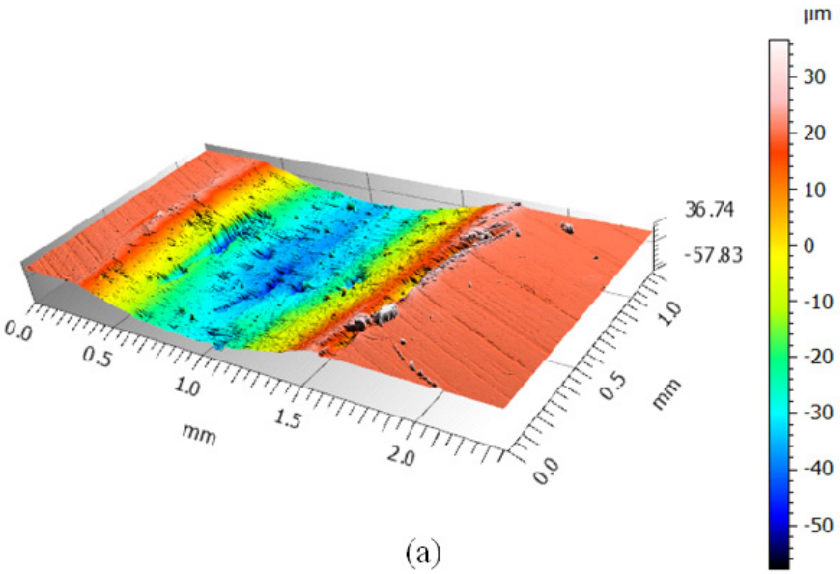


(a)

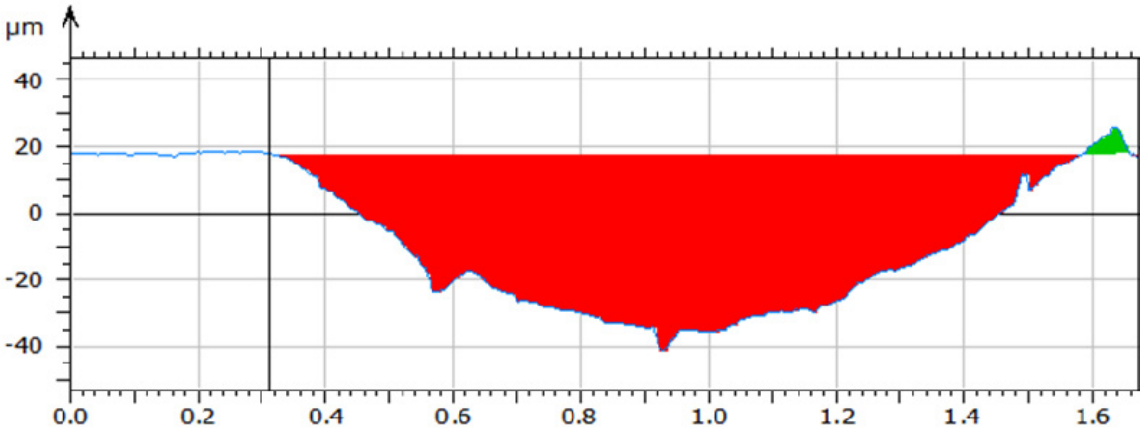


| Parameters | Value | Unit |
|---|---|---|
| Maximum depth | 59.76 | µm |
| Hole area | 43977 | µm² |

(b)

**Figure 12.** Surface texture topography of the composite containing 2.5% of T15 HSS steel particles after tribological tests under technically dry friction: (a) isometric image, (b) surface profile.

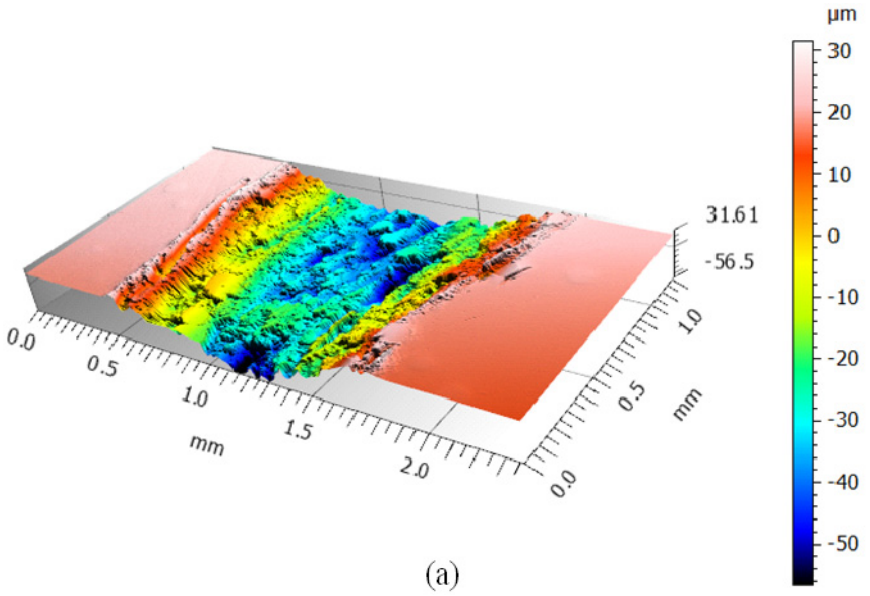


(a)

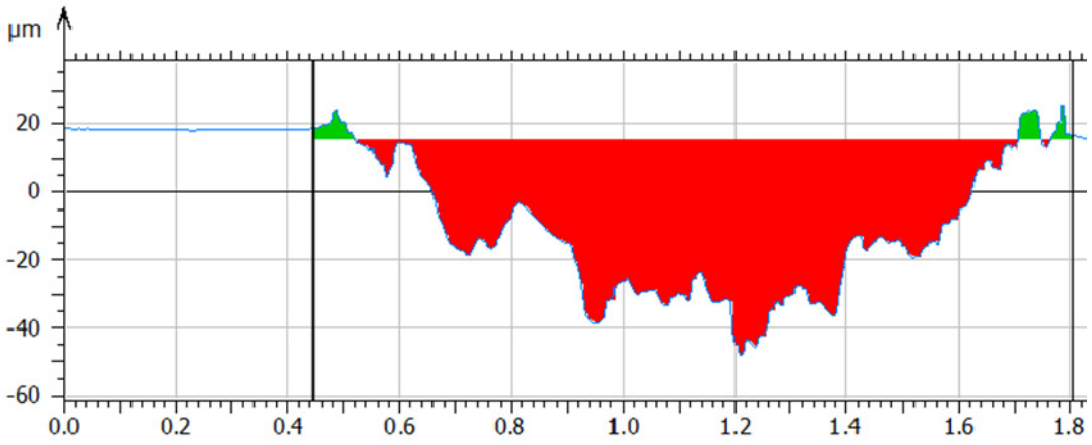


| Parameters | Value | Unit |
|---|---|---|
| Maximum depth | 64.09 | µm |
| Hole area | 38756 | µm² |

(b)

**Figure 13.** Surface texture topography of the composite containing 5% of T15 HSS steel particles after tribological tests under technically dry friction: (a) isometric image, (b) surface profile.

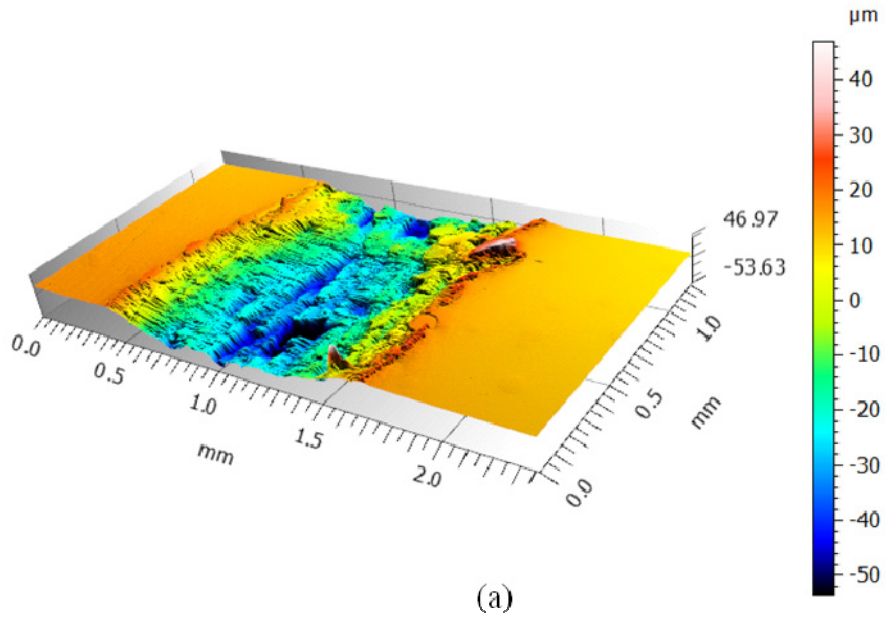


(a)

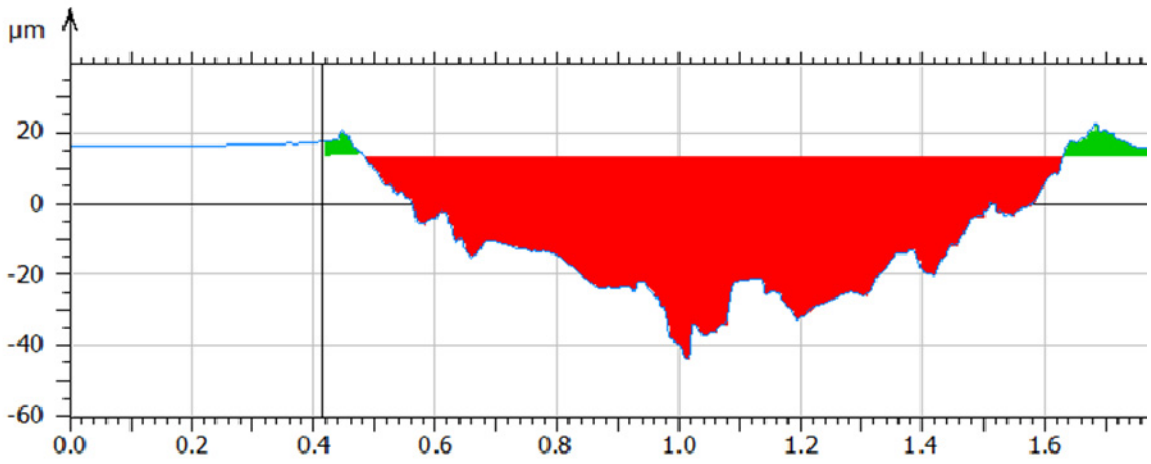


| Parameters | Value | Unit |
|---|---|---|
| Maximum depth | 58.32 | µm |
| Hole area | 34997 | µm² |

(b)

**Figure 14.** Surface texture topography of the composite containing 7.5% of T15 HSS steel particles after tribological tests under technically dry friction: (a) isometric image, (b) surface profile.

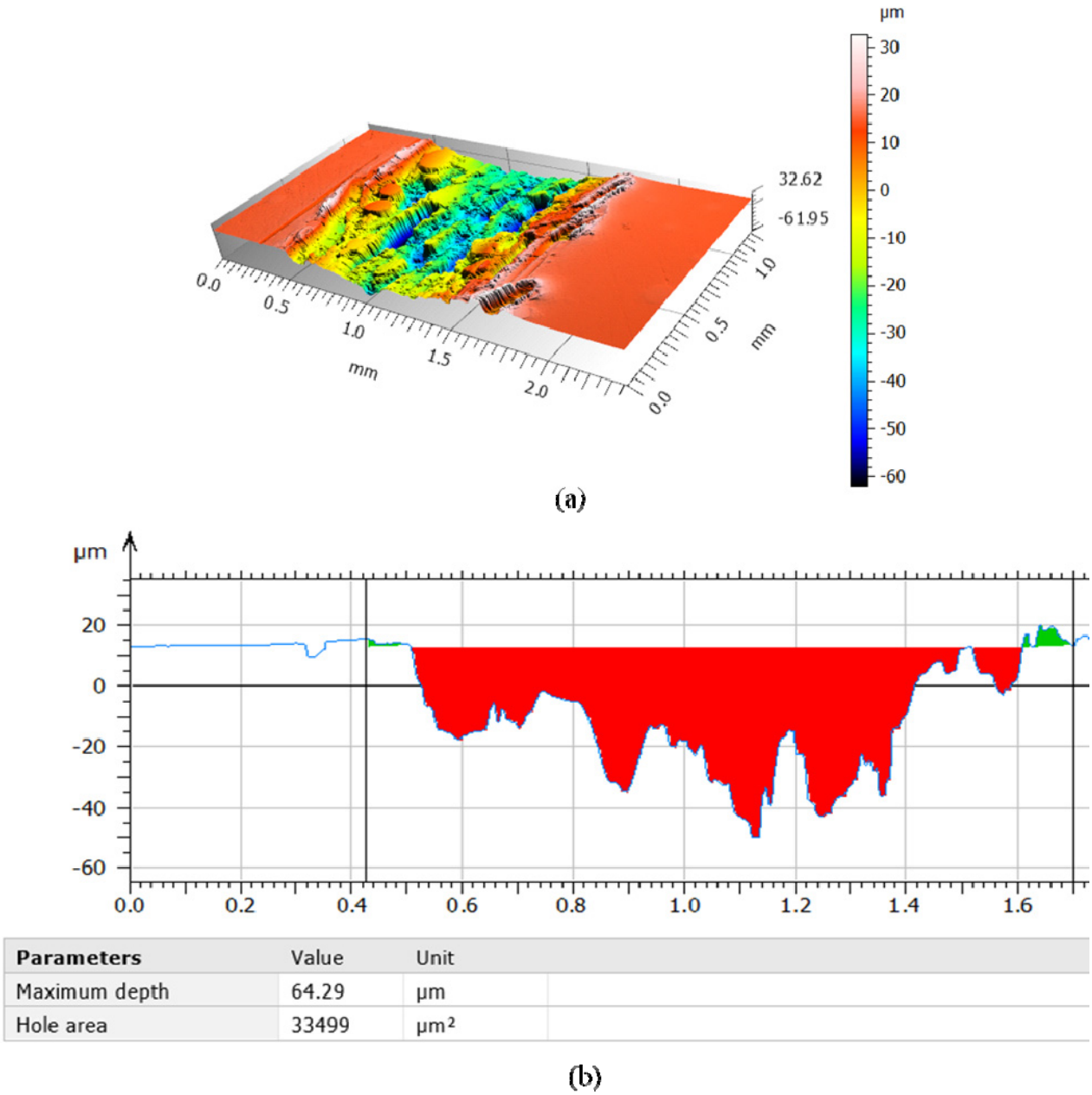


**Figure 15.** Surface texture topography of the composite containing 10% of T15 HSS steel particles after tribological tests under technically dry friction: (a) isometric image, (b) surface profile.

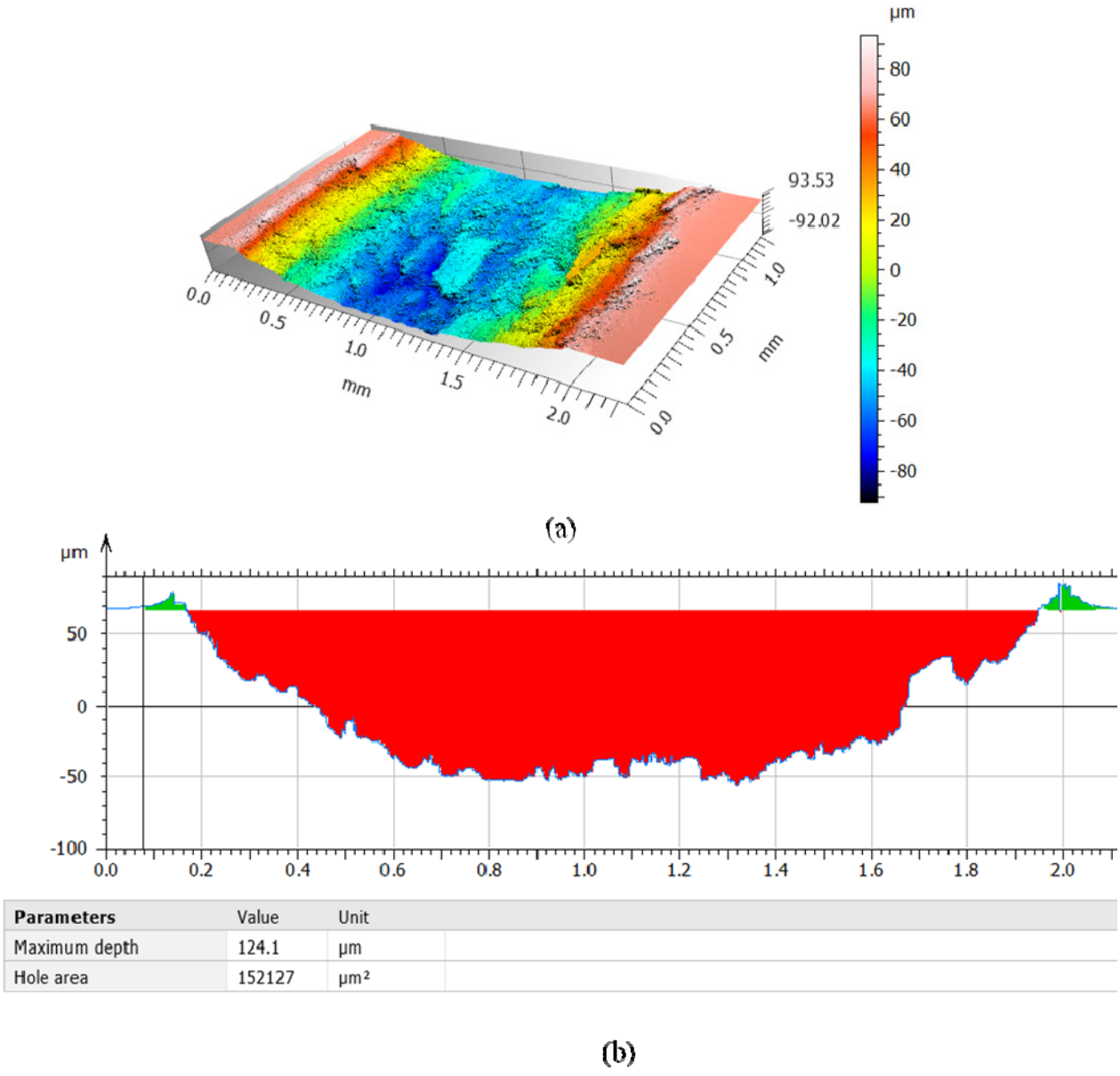


**Figure 16.** Surface texture topography of the composite containing 2.5% of carbon steel particles after tribological tests under technically dry friction: (a) isometric image, (b) surface profile.

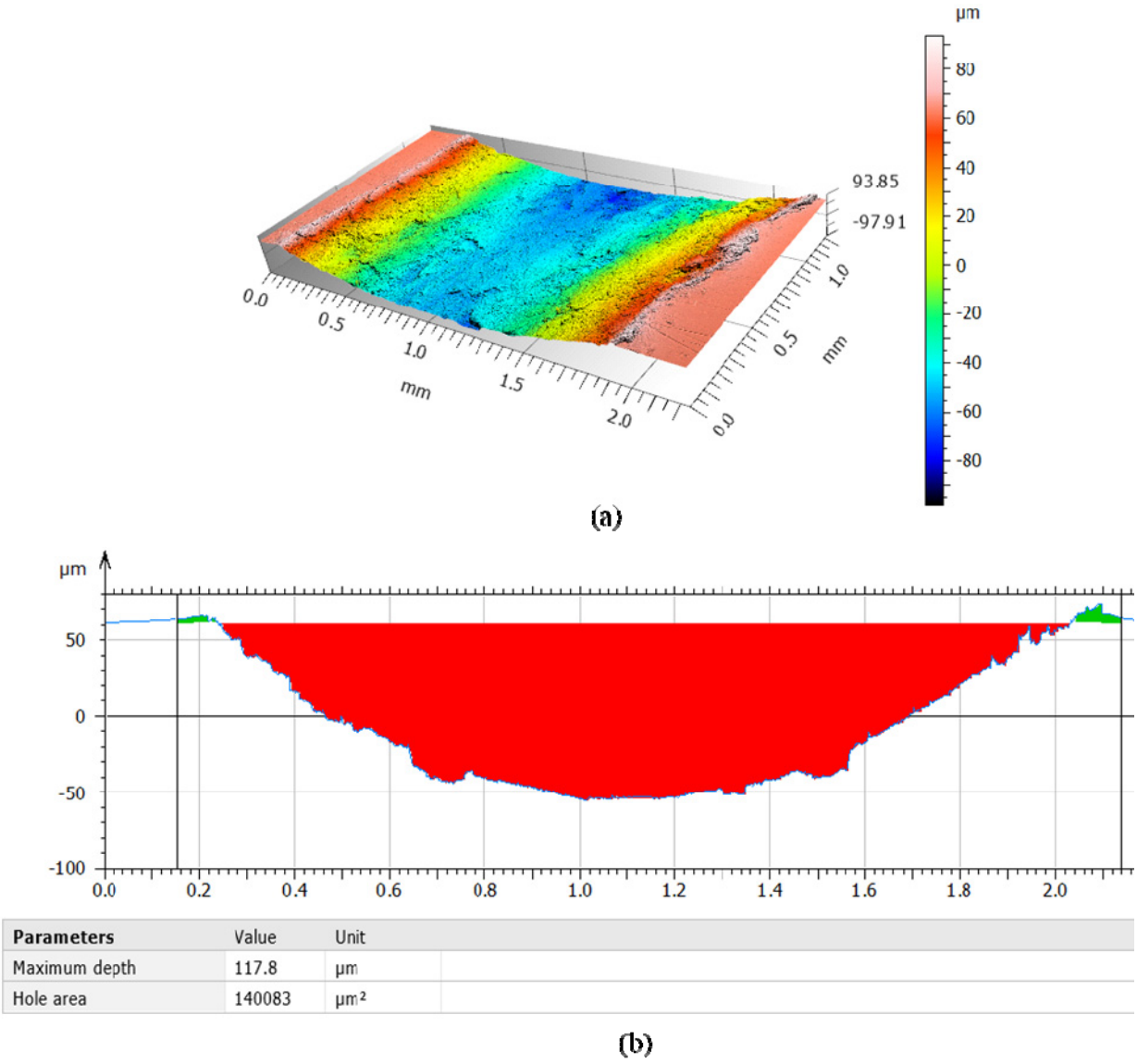


**Figure 17.** Surface texture topography of the composite containing 5% of carbon steel particles after tribological tests under technically dry friction: (a) isometric image, (b) surface profile.

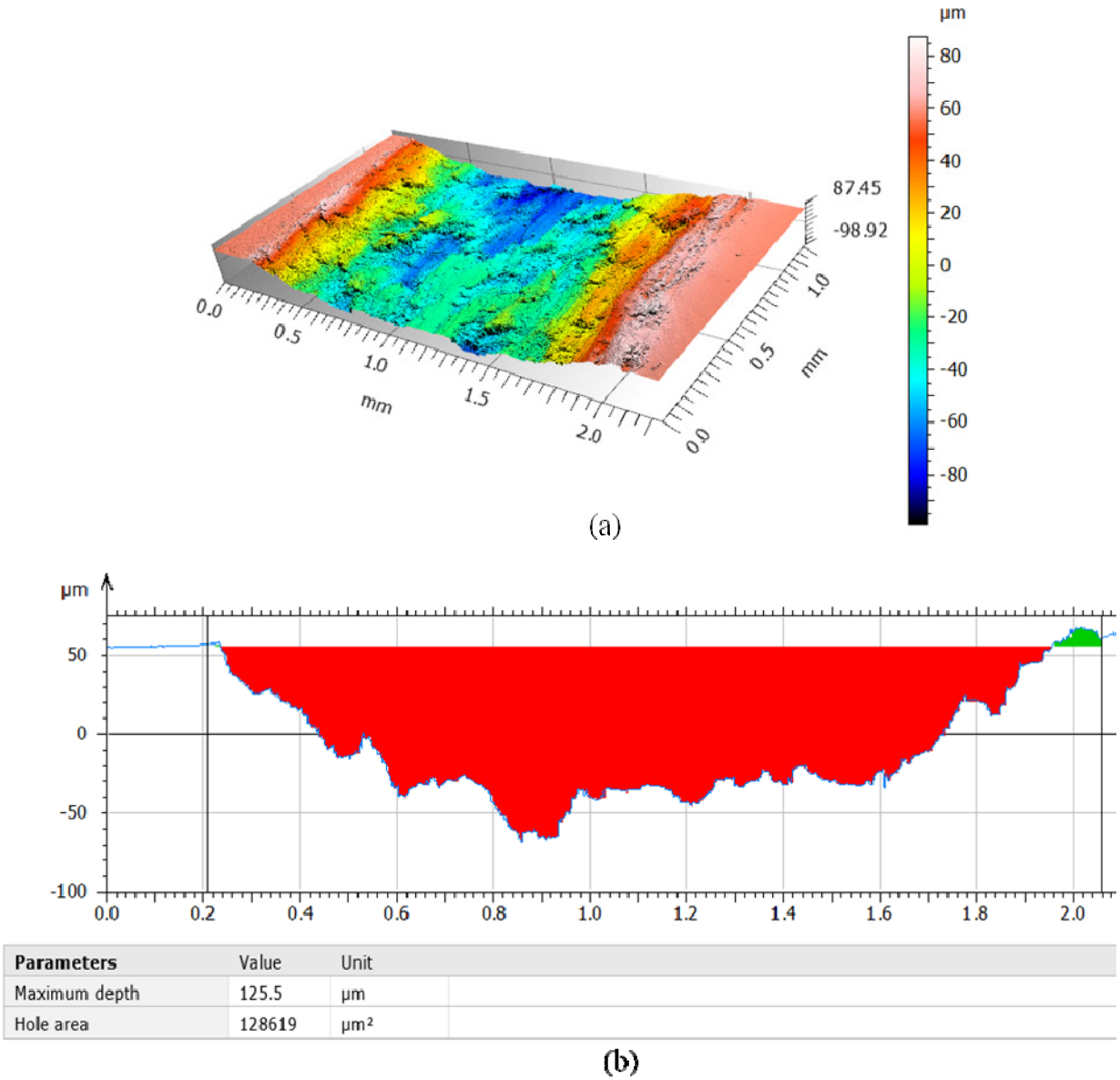


**Figure 18.** Surface texture topography of the composite containing 7.5% of carbon steel particles after tribological tests under technically dry friction: (a) isometric image, (b) surface profile.

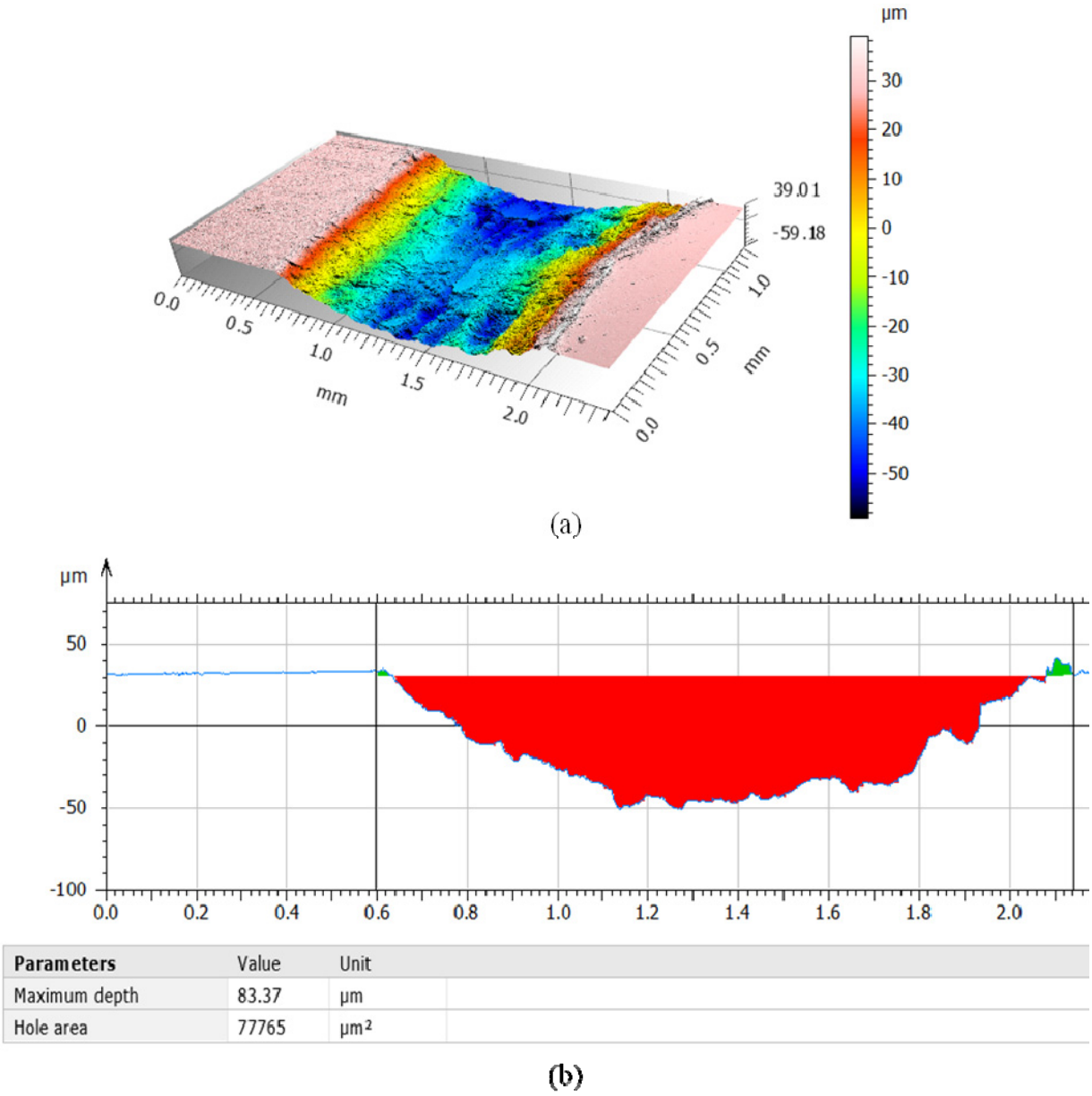


**Figure 19.** Surface texture topography of the composite containing 10% of carbon steel particles after tribological tests under technically dry friction: (a) isometric image, (b) surface profile.

The analysis of the geometric structure of the surface confirmed the results obtained during the tests of abrasive wear resistance of the composites. The lowest wear was observed for the composite containing 10% of the T15 high-speed steel powder. While observing the structures, it is possible to notice the places where the steel particles were pulled out of the copper matrix. The test results show that the high-speed steel particles have a better bond with the copper matrix compared to the carbon steel particles. As the carbon steel particles were pulled out of the copper matrix, greater friction resulted in greater abrasive wear.

## 4. Conclusions

Examination of the microstructure of the fabricated copper matrix composites reinforced with steel particles showed that the steel particles aggregate into agglomerates. To obtain an even distribution of strengthening particles in the copper matrix, the powders should be thoroughly mixed before the pressing process. A uniform distribution of the particles is necessary to obtain the same properties throughout the sinters volume. Based on the observation of the microstructure, it should be concluded that the parameters of the composite manufacturing process were selected correctly. Microstructure studies have shown that the reinforcement particles are well bonded to the copper matrix, especially T15 high speed steel particles, which can be seen in Figures 6,7. The pores characteristics of sintered products are visible in the structure of the sintered composites. The introduction of steel particles increased the hardness of the composites. Both for carbon steel and high-speed steel, the hardness values are not significant. The density of composites decreases as the amount of steel particles in the copper matrix increases. The introduction of steel particles into the copper matrix reduces the electrical conductivity. For composites reinforced with high-speed steel particles, satisfactory results of electrical conductivity were obtained. It is related to the lack of diffusion between the copper matrix and the high-speed steel particles. Tribological tests of the produced composites showed that the introduction of high-speed steel particles increases their resistance to abrasive wear. The introduction of carbon steel particles caused a deterioration of the abrasive wear resistance. This is due to the carbon steel particles being pulled out of the matrix during friction. The shape and size of the strengthening particles also have an influence on the wear resistance. All tests carried out have shown that the high-speed steel particles used as reinforcing particles have better properties than carbon steel particles.

## Acknowledgements

This research did not receive any specific grant from funding agencies in the public, commercial, or not-for-profit sectors.

## Conflict of interests

The authors declare no conflict of interests.

## References

1. Islak S, Kur D, Buytoz S (2014) Effect of sintering temperature on electrical and microstructure properties of hot pressed Cu–TiC composites. *Sci Sinter 46*: 15–21.
2. Mikuła J, Łach M, Kowalski JS (2015) Copper matrix composites reinforced with volcanic tuff. *Metalurgija* 54: 143–146.
3. Kruger C, Mortensen A (2013) *In situ* copper–alumina composites. *Mater Sci Eng A-Struct* 585: 396–407.
4. Kargul M, Konieczny M, Borowiecka-Jamrozek J (2018) The effect of the addition of zeolite particles one the performance characteristics of sintered copper matrix composites. *Tribologia* 6: 51–62.

5. Kargul M, Konieczny M (2020) Fabrication and characteristics of copper-intermetallics composites. *Arch Foun Eng* 20: 25–30.
6. Semboshi S, Takasugi T (2013) Fabrication of high-strength and high-conductivity Cu–Ti alloy wire by aging in a hydrogen atmosphere. *J Alloy Compd* 580: 397–400.
7. Konieczny M, Dziadoń A, Mola R (2006) Structure Of copper-intermetallics composite sintered from copper and titanium powders. *2-nd International Conference Engineering and Education*, 89–94.
8. Taha MA, Zawrah MF (2017) Effect of nano $ZrO_2$ on strengthening and electrical properties of Cu-matrix nanocomposites prepared by mechanical alloying. *Ceram Int* 43: 12698–12704.
9. Garzon-Manjon A, Christiansen L, Kirchlechner I, et al. (2019) Synthesis, microstructure and hardness of rapidly soldified Cu–Cr alloys. *J Alloy Compd* 794: 203–209.
10. Samal CP, Parihar JS, Chaira D (2013) The effect of milling and sintering techniques on mechanical properties of Cu-graphite metal matrix composite prepared by powder metallurgy route. *J Alloy Compd* 569: 95–101.
11. Wang C, Lin H, Zhang Z, et al. (2018) Fabrication, interfacial characteristics and strengthening mechanism of $ZrB_2$ microparticles reinforced Cu composites prepared by hot pressing sintering. *J Alloy Compd* 748: 546–552.
12. Fathy A, Elkady O, Abu-Oqail A (2017) Synthesis and characterization of Cu–$ZrO_2$ nanocomposite produced by thermochemical process. *J Alloy Compd* 719: 411–419.
13. Fathy A (2018) Investigation on microstructure and properties of Cu–$ZrO_2$ nanocomposites synthesized by in situ processing. *Mater Lett* 213: 95–99.
14. Shojaeepour F, Abachi P, Purazrang K, et al. (2012) Production and properties of Cu/$Cr_2O_3$ nano-composites. *Powder Technol* 222: 80–84.
15. Bahador A, Umeda J, Yamanoglu R, et al. (2020) Deformation mechanism and enhanced properties of Cu–$TiB_2$ composites evaluated by the in situ tensile test and microstructure characterization. *J Alloy Compd* 847: 156555.
16. Bahador A, Umeda J, Hamzah E, et al. (2020) Synergistic strengthening mechanism of copper matrix composites with $TiO_2$ nanoparticles. *Mater Sci Eng A-Struct* 772: 138797.
17. Konieczny M, Mola R (2007) Sintered copper matrix composites containing aluminium-ferric intermetallic phases. *Composites* 7: 109–113.
18. Jóźwik P, Polkowski W, Bojar Z (2015) Applications of $Ni_3Al$ based intermatallic alloys-current stage and potential perceptivities. *Materials* 8: 2537–2568.
19. Hayama AOF, Andrade PN, Cremasco, A, et al. (2014) Effects of composition and heat treatment on the mechanical behavior of Ti–Cu alloys. *Mater Design* 55: 1006–1013.
20. Karakulak E (2017) Characterization of Cu–Ti powder metallurgical materials. *Int J Min Met Mater* 4: 83–90.
21. Semboshi , Niskida, T, Namakura H (2009) Microstructure and mechanical properties of Cu–3 at% Ti alloy aged in a hydrogen atmosphere. *Mater Sci Eng A-Struct* 517: 105–113.
22. El-Rakayby AM, Mills B (1988) On the microstructure and mechanical properties of high-speed steels. *J Mater Sci* 23: 4340–4344.
23. Varez A, Portuondo J, Levenfeld B, et al. (2001) Processing of P/M high speed steels by mould casting using thermosetting binders. *Mater Chem Phys* 67: 43–48.

24. Zhang G, Yuan H, Jiao D, et al. (2012) Microstructure evolution and mechanical properties of T15 high speed steel prepared by twin atomiser spray forming and thermos mechanical processing. *Mater Sci Eng A-Struct* 558: 565–571.
25. Serna MM, Jesus ERB, Galego E, et al. (2006) An overview of the microstructure present in high speed steel carbides crystallography. *Mater Sci Forum* 530: 48–52.
26. Turel A, Slavic J, Boltezar H, et al. (2017) Electrical contact resistance and wear of a dynamically excited metal-graphite brush. *Adv Mech Eng* 9: 1–8.
27. Turel A, Slavic J, Boltezar H (2018) Wear rate vs dynamic and material properties at elevated temperatures for a copper graphite brush. *Stroj Vestn-J Mech E* 64: 169–175.


AIMS Press